

# Bayesian Optimization for Personalized Dose-Finding Trials with Combination Therapies

James Willard<sup>1,\*</sup>, Shirin Golchi<sup>1</sup>, Erica E.M. Moodie<sup>1</sup>,  
Bruno Boulanger<sup>2</sup>, and Bradley P. Carlin<sup>2</sup>

<sup>1</sup>McGill University, Montreal, Canada

<sup>2</sup>PharmaLex, Mont-Saint-Guibert, Belgium

## Abstract

Identification of optimal dose combinations in early phase dose-finding trials is challenging, due to the trade-off between precisely estimating the many parameters required to flexibly model the dose-response surface, and the small sample sizes in early phase trials. Existing methods often restrict the search to pre-defined dose combinations, which may fail to identify regions of optimality in the dose combination space. These difficulties are even more pertinent in the context of personalized dose-finding, where patient characteristics are used to identify tailored optimal dose combinations. To overcome these challenges, we propose the use of Bayesian optimization for finding optimal dose combinations in standard (“one size fits all”) and personalized multi-agent dose-finding trials. Bayesian optimization is a method for estimating the global optima of expensive-to-evaluate objective functions. The objective function is approximated by a surrogate model, commonly a Gaussian process, paired with a sequential design strategy to select the next point via an acquisition function. This work is motivated by an industry-sponsored problem, where focus is on optimizing a dual-agent therapy in a setting featuring minimal toxicity. To compare the performance of the standard and personalized methods under this setting, simulation studies are performed for a variety of scenarios. Our study concludes that taking a personalized approach is highly beneficial in the presence of heterogeneity.

# 1 Introduction

Early phase clinical trials are designed to assess the safety and efficacy profiles of first in human doses of an experimental drug. Traditional adaptive dose-finding designs fall into three major families: algorithmic designs, model-assisted designs, and model-based designs (Berry et al., 2010). Here, our interest lies in model-based designs, which have been extended to the dual-agent dose combination setting (e.g., Wang and Ivanova 2005; Wages and Conaway 2014). While some of these designs (e.g., Houede et al. 2010; Wang et al. 2023) recognize that monotonicity between dose and both efficacy and toxicity may not hold in general (Li et al., 2017), they restrict dose-finding to a set of pre-selected dose combinations, which can fail to identify the optimal dose combination (Hirakawa et al., 2015). Adaptive dose insertion designs have been proposed to allow for the evaluation of additional dose combinations if warranted by the data (Cai et al., 2014; Lyu et al., 2019).

Most of the existing dose-finding designs, including those mentioned above, seek to find optimal dose combinations without consideration of additional covariate information (we refer to this as *standard dose-finding*). These designs ignore the possibility that patient responses may be quite variable across different groups of individuals within the population. With recent advances in molecular biology, specifically the identification of novel biomarkers, interest has grown in personalized (or precision) medicine. *Personalized dose-finding* aims to find optimal dose combinations based on individual patient characteristics. When utilizing parametric models, as in many of the standard dose-finding methods described above, extension to the personalized setting is challenging due to the limited sample sizes and potentially large number of dose-covariate interaction terms required. For single-agent personalized dose-finding, dimension-reduction methods have been proposed (Guo and Zang, 2022). Mozgunov et al. (2022) has considered dual-agent personalized dose-finding, but where the patient-specific dose of one of the agents is selected externally by clinicians. To the authors' knowledge, there are currently no multi-agent personalized dose-finding designs where all dose dimensions are explored during optimization.

Our work is motivated by a problem in industry, where a sponsor is interested in a design for the development of an intraocular implant that combines two topical agents. Each agent has

been in use for many years and is well tolerated. No drug-related adverse events are expected, and we assume minimal toxicity, if any. Interest lies in obtaining the optimal dose combination of these two agents using a continuous efficacy measure, which need not be monotonic with the doses of each agent. Additionally, response heterogeneity is expected to exist with respect to a key binary covariate, a particular characteristic of the lens of the eye, and we are interested in a design which accommodates this feature. We allow for exploration of the entire continuous candidate dose combination region, which has been defined using data from previous observational and randomized studies. As each new dose combination investigated carries engineering costs, early stopping is desirable if warranted by the data.

Considering this motivating example, we propose novel methodology for multi-agent dose-finding which meets several criteria. First, the model estimating the response surface is parsimonious, which is suitable for small sample sizes, yet remains flexible enough to model non-monotonic dose-response surfaces. Next, the design sequentially explores the entire dose combination space in a principled way, and allows for early stopping if warranted. Finally, our methodology facilitates extension to personalized dose-finding. Specifically, we propose modelling the response surface with a Gaussian process (GP) and using Bayesian optimization methods for efficient standard and personalized multi-agent dose-finding, assuming minimal toxicity.

The remainder of this manuscript is organized in the following manner. In Section 2, we introduce Bayesian optimization, propose methods for standard and personalized multi-agent dose-finding, and propose an early stopping rule. In Section 3, we perform a simulation study to compare the standard and personalized dose-finding methods for a dual-agent therapy under a variety of scenarios without early stopping. In Section 4, we consider the development of the previously described intraocular implant and compare several dose-finding designs which include early stopping rules. Finally, Section 5 offers a closing discussion and possible directions for future work.

## 2 Bayesian Optimization for Dose-Finding

### 2.1 Standard Dose-Finding

Define  $f^\dagger(\mathbf{d})$  to be a continuous dose-response surface of interest. This may be the dose-efficacy surface or the dose-utility surface, where utility is defined using both efficacy and toxicity outcomes. For the remainder of the manuscript, we assume  $f^\dagger(\mathbf{d})$  is the dose-efficacy surface, though we note that all proposed methods apply to the dose-utility setting. We assume minimal toxicity, i.e., a tolerated toxicity level is presumed over the entire dose combination space,  $\mathbb{D}$ . Thus, dose escalation/de-escalation rules are not considered, and it is ethically permissible to select future dose combinations throughout the design space. Our interest is in obtaining the combination of  $J$  dosing agents  $\mathbf{d} = (d_1, \dots, d_J) \in \mathbb{D} \subset \mathbb{R}^J$  which maximizes  $f^\dagger(\mathbf{d})$ . That is, the search for the optimal dose combination is not to be restricted to a set of pre-defined doses, but rather a subspace of  $\mathbb{R}^J$ . Since optimization problems are commonly viewed as minimizing an objective function, we note that the objective function  $f(\mathbf{d})$  for  $f^\dagger(\mathbf{d})$  can be defined as:

$$f(\mathbf{d}) = \begin{cases} -f^\dagger(\mathbf{d}) & \text{if positive values of } f^\dagger(\mathbf{d}) \text{ are preferred} \\ f^\dagger(\mathbf{d}) & \text{otherwise.} \end{cases}$$

Then the goal is to identify the optimal dose combination:

$$\underset{\mathbf{d} \in \mathbb{D}}{\operatorname{argmin}} f(\mathbf{d}).$$

To obtain the optimal dose combination, Bayesian optimization can be utilized. Bayesian optimization is a derivative-free optimization method that estimates the global optima of expensive-to-evaluate objective functions (Garnett, 2023). It is a sequential design strategy that approximates the objective function with a stochastic surrogate model (commonly a GP), and selects the next point by optimizing a so-called acquisition function. Bayesian optimization is commonly used in engineering, machine learning, and computer experiments (Gramacy, 2020; Murphy, 2023), and has recently been employed to efficiently find optimal dynamic treatment regimes (Duque et al.,

2022; Freeman et al., 2022). We use it in this manuscript by modeling the objective function with a GP, and by selecting the next dose combination as that which maximizes an acquisition function. This process repeats until optimality criteria are satisfied or sample size limits are reached.

To optimize  $f(\mathbf{d})$ ,  $r$  patients are assigned to each of  $c$  initial dose combinations, yielding  $n = r \times c$  patient responses which are treated as noisy observations  $y_i = f(\mathbf{d}_i) + \epsilon_i$ , where  $\epsilon_i \sim N(0, \sigma_y^2)$  for  $i = 1, \dots, n$ . A GP prior is then placed on the latent objective function,

$$f(\mathbf{d}) \sim GP(m(\mathbf{d}), \mathcal{K}(\mathbf{d}, \mathbf{d}'))$$

where  $m(\mathbf{d}) = \mathbb{E}[f(\mathbf{d})]$  is the mean function, and  $\mathcal{K}(\mathbf{d}, \mathbf{d}') = [(f(\mathbf{d}) - m(\mathbf{d}))(f(\mathbf{d}') - m(\mathbf{d}'))^T]$  is a covariance function with a positive definite kernel (Williams and Rasmussen, 2006). While information about the response surface (e.g., pharmacokinetic/pharmacodynamic models) can be incorporated through the mean function, in the absence of information, constant mean GPs can be used. For standardized outcomes, GP models with zero-mean functions  $m(\mathbf{d}) = 0$  are commonly used since the method’s flexibility is largely determined by the choice of kernel function. In this work we employ an anisotropic squared exponential kernel:

$$\mathcal{K}(\mathbf{d}, \mathbf{d}') = \sigma_f^2 \exp \left\{ - \sum_{j=1}^J \frac{(d_j - d'_j)^2}{2l_{d_j}^2} \right\}. \quad (1)$$

This kernel is parameterized by a scale parameter  $\sigma_f^2$ , which determines the variability of the objective function throughout the dose combination space, and characteristic length-scales  $l_{d_j}$ , which control the rate of decay in correlation between two dose combinations with respect to each dosing dimension. The squared exponential kernel is an example of a stationary kernel, which assumes the degree of correlation between two dose combinations depends only on their distance from one another, not on their locations in the dose combination space. This induces a multivariate normal distribution on the observations,

$$\mathbf{y} \sim N(\mathbf{0}, \mathbf{K}_{D,D} + \sigma_y^2 \mathbf{I}_n)$$

with positive definite covariance matrix  $\mathbf{K}_{D,D}(i, j) = \mathcal{K}(\mathbf{d}_i, \mathbf{d}_j)$ . After observing data  $\mathcal{D} = \{(\mathbf{d}_i, y_i)\}_{i=1}^n$ , we adopt an empirical Bayes approach toward the kernel hyperparameters  $\boldsymbol{\theta} = \{\sigma_f^2, \sigma_y^2, l_{d_1}, l_{d_2}\}$ , by replacing them with their maximum likelihood estimates. Performing hyperparameter inference via empirical Bayes is common in the machine learning and computer experiments literature (Williams and Rasmussen, 2006; Gramacy, 2020). The posterior distribution of  $\mathbf{f}$  at a set of new dose combinations  $\tilde{\mathbf{D}}$  is then multivariate Student- $t$  (denoted by  $\mathcal{T}$ ) with  $\nu = n$  degrees of freedom, mean vector  $\tilde{\boldsymbol{\mu}}$ , and scale matrix  $\tilde{\boldsymbol{\Sigma}}$  (Gramacy, 2016):

$$p(\mathbf{f} \mid \mathcal{D}, \tilde{\mathbf{D}}) = \mathcal{T}(\tilde{\boldsymbol{\mu}}, \tilde{\boldsymbol{\Sigma}}, \nu)$$

such that

$$\begin{aligned} \tilde{\boldsymbol{\mu}} &= \mathbf{K}_{D, \tilde{D}}^T (\mathbf{K}_{D,D} + \sigma_y^2 \mathbf{I}_n)^{-1} \mathbf{y} \\ \tilde{\boldsymbol{\Sigma}} &= \frac{\mathbf{y}^T (\mathbf{K}_{D,D} + \sigma_y^2 \mathbf{I}_n)^{-1} \mathbf{y} \left[ \mathbf{K}_{\tilde{D}, \tilde{D}} - \mathbf{K}_{D, \tilde{D}}^T (\mathbf{K}_{D,D} + \sigma_y^2 \mathbf{I}_n)^{-1} \mathbf{K}_{D, \tilde{D}} \right]}{\nu} \end{aligned}$$

where  $\mathbf{K}_{D,D}$  is  $n \times n$ ,  $\mathbf{K}_{D, \tilde{D}}(i, j) = \mathcal{K}(\mathbf{d}_i, \tilde{\mathbf{d}}_j)$  is  $n \times n_{\tilde{D}}$ , and  $\mathbf{K}_{\tilde{D}, \tilde{D}}(i, j) = \mathcal{K}(\tilde{\mathbf{d}}_i, \tilde{\mathbf{d}}_j)$  is  $n_{\tilde{D}} \times n_{\tilde{D}}$ . We note the posterior covariance matrix is  $\text{Cov}(\mathbf{f} \mid \mathcal{D}, \tilde{\mathbf{D}}) = \tilde{\boldsymbol{\Sigma}} \times \nu / (\nu - 2)$ . The next dose combination for evaluation, denoted by  $\mathbf{d}^{(c+1)}$ , is then selected as that candidate dose combination  $\tilde{\mathbf{d}} \in \mathbb{D}$  which maximizes an acquisition function,  $\alpha(\tilde{\mathbf{d}} \mid \mathcal{D})$ :

$$\mathbf{d}^{(c+1)} = \underset{\tilde{\mathbf{d}} \in \mathbb{D}}{\text{argmax}} \alpha(\tilde{\mathbf{d}} \mid \mathcal{D}).$$

One acquisition function commonly paired with a GP is the Expected Improvement (EI), defined as

$$\alpha_{EI}(\tilde{\mathbf{d}} \mid \mathcal{D}) = \mathbb{E}[\max(0, f^* - f(\tilde{\mathbf{d}})) \mid \mathcal{D}, \tilde{\mathbf{d}}]$$

and available in closed form (Jones et al., 1998),

$$\alpha_{EI}(\tilde{\mathbf{d}} \mid \mathcal{D}) = (f^* - \mu(\tilde{\mathbf{d}})) \Phi \left( \frac{f^* - \mu(\tilde{\mathbf{d}})}{\sigma(\tilde{\mathbf{d}})} \right) + \sigma(\tilde{\mathbf{d}}) \phi \left( \frac{f^* - \mu(\tilde{\mathbf{d}})}{\sigma(\tilde{\mathbf{d}})} \right),$$

where  $f^*$  denotes the current optimum,  $\Phi(\cdot)$  and  $\phi(\cdot)$  denote the cdf and pdf of a standard normal

random variable, respectively, and where  $\mu(\tilde{\mathbf{d}})$  and  $\sigma(\tilde{\mathbf{d}})$  are the posterior mean and standard deviation of  $f$  evaluated at  $\tilde{\mathbf{d}}$ , respectively. From above, we see that the EI balances the trade-off between *exploiting* regions that have desirable values of  $f(\mathbf{d})$  (first term), and *exploring* regions in the dose combination space that are imprecisely estimated (second term). Under a noisy setting, we set  $f^* = \min_{\mathbf{d}} \tilde{\boldsymbol{\mu}}$ , the minimum of the posterior mean (Gramacy and Lee, 2010; Picheny et al., 2013). After evaluation of  $\mathbf{d}^{(c+1)}$  in  $r$  new patients, the data are updated,  $\mathcal{D} = \mathcal{D} \cup \{(\mathbf{d}_i^{(c+1)}, y_i)\}_{i=1}^r$ . The GP model is refit to obtain a new posterior distribution  $p(\mathbf{f} \mid \mathcal{D}, \tilde{\mathbf{D}})$ . Then  $s = 1, \dots, S$  samples  $f_s(\tilde{\mathbf{d}})$  from this posterior are obtained to yield  $S$  samples from the posterior of the optimal dose combination  $p(\mathbf{d}_{opt} \mid \mathcal{D})$  as:

$$\mathbf{d}_{opt,s} = \underset{\tilde{\mathbf{d}} \in \mathbb{D}}{\operatorname{argmin}} f_s(\tilde{\mathbf{d}}).$$

This procedure continues until the sample size limit is reached or an early stopping rule, which we denote by  $\mathbb{1}_{\text{STOP}}$ , is satisfied.

One possible early stopping rule is to allow stopping only after  $\max_{\tilde{\mathbf{d}} \in \mathbb{D}} \alpha_{EI}(\tilde{\mathbf{d}} \mid \mathcal{D}) < \delta$ . In this case, the algorithm terminates only if there is little improvement to be gained over  $f^*$  across the dose combination space. Additionally, a minimum stopping sample size  $n_{\text{STOP}}$  can be set, such that  $n_{\text{STOP}} > n_0$ , where  $n_0$  is the number of participants assigned to the initial dose combinations. This guarantees some exploration of the dose combination space after having evaluated the initial dose combinations, and yields the following stopping rule:

$$\mathbb{1}_{\text{STOP}} = \begin{cases} \text{TRUE} & n \geq n_{\text{STOP}} \text{ and } \max_{\tilde{\mathbf{d}} \in \mathbb{D}} \alpha_{EI}(\tilde{\mathbf{d}} \mid \mathcal{D}) < \delta \\ \text{FALSE} & \text{otherwise.} \end{cases} \quad (2)$$

We note that both  $n_{\text{STOP}}$  and  $\delta$  are tuning parameters that help control performance of the algorithms. Their values can be determined through Monte Carlo simulations. For example, a set of Monte Carlo simulations using the maximum sample size can be performed. Using these, the Monte Carlo distributions of  $\alpha_{EI}$  by iteration can be obtained. Then, a statistic (e.g., the median) of each  $\alpha_{EI}$  distribution can be set as  $\delta$ , and the corresponding sample size at that iteration set as  $n_{\text{STOP}}$ . Finally, several combinations of  $n_{\text{STOP}}$  and  $\delta$  can be selected, and their performance

---

**Algorithm 1** Standard Optimization Algorithm

---

**Require:**  $r$  patient responses at each of  $c$  initial dose combinations,  $\mathcal{D} = \{(\mathbf{d}_i, y_i)\}_{i=1}^{n_0}$

- 1:  $n \leftarrow n_0 = r \times c$
- 2:  $\mathbb{1}_{\text{STOP}} \leftarrow \text{FALSE}$
- 3: Obtain  $p(\mathbf{f} \mid \mathcal{D}, \tilde{\mathbf{D}})$  and  $p(\mathbf{d}_{\text{opt}} \mid \mathcal{D})$  using fitted GP ▷ Obtain posteriors
- 4:  $f^* \leftarrow \min_{\mathbf{d}} \tilde{\boldsymbol{\mu}}$  ▷ Obtain best value of  $f$
- 5: Calculate  $\alpha_{EI}(\tilde{\mathbf{d}} \mid \mathcal{D})$  for  $\tilde{\mathbf{d}} \in \mathbb{D}$  ▷ Compute EI
- 6: **while**  $n < N$  and  $\mathbb{1}_{\text{STOP}} = \text{FALSE}$  **do**
- 7:      $\mathbf{d}^{(c+1)} \leftarrow \operatorname{argmax}_{\tilde{\mathbf{d}} \in \mathbb{D}} \alpha_{EI}(\tilde{\mathbf{d}} \mid \mathcal{D})$  ▷ Obtain next dose
- 8:     **for**  $i = 1, \dots, r$  **do**
- 9:         Evaluate  $y_i$  at  $\mathbf{d}^{(c+1)}$  ▷ Observe outcomes
- 10:     **end for**
- 11:      $n \leftarrow n + r$  ▷ Update  $n$
- 12:      $\mathcal{D} \leftarrow \mathcal{D} \cup \{(\mathbf{d}_i^{(c+1)}, y_i)\}_{i=1}^r$  ▷ Update data
- 13:     Obtain  $p(\mathbf{f} \mid \mathcal{D}, \tilde{\mathbf{D}})$  and  $p(\mathbf{d}_{\text{opt}} \mid \mathcal{D})$  using fitted GP ▷ Obtain posteriors
- 14:      $f^* \leftarrow \min_{\mathbf{d}} \tilde{\boldsymbol{\mu}}$  ▷ Obtain best value of  $f$
- 15:     Calculate  $\alpha_{EI}(\tilde{\mathbf{d}} \mid \mathcal{D})$  for  $\tilde{\mathbf{d}} \in \mathbb{D}$  ▷ Compute EI
- 16:     Update  $\mathbb{1}_{\text{STOP}}$  using (2) ▷ Update stopping rule
- 17: **end while**

---

assessed through simulation.

The sequential procedure and stopping rule described above suggest Algorithm 1, referred to as the *standard optimization algorithm*. In many applications of Bayesian optimization, it is standard to collect the initial data and then continue with  $r = 1$  at each iteration of the algorithm. This permits maximal exploration of the domain, as a novel input point from the design space can be evaluated each time. In certain dose-finding applications, such as the motivating example of this work, engineering costs may prohibit the creation of a novel dose combination for each new patient, and some patients may necessarily be assigned to the same dose.

## 2.2 Personalized Dose-Finding

Personalized medicine recognizes that response heterogeneity may exist within the population of interest, and so personalized dose-finding should incorporate covariate information to account for this. Consider a set of  $P$  discrete covariates  $\mathbf{Z} = \{Z_p\}_{p=1}^P$ . The Cartesian product of the levels of these  $P$  covariates define  $K$  strata. The goal of personalized dose finding is to find the optimal

dose combinations across the continuous dose combination space for each of the  $K$  strata:

$$\operatorname{argmin}_{\mathbf{d} \in \mathbb{D}} f(\mathbf{d}, \mathbf{z}_k) \quad \text{for } k = 1, \dots, K.$$

The objective function  $f(\mathbf{d}, \mathbf{z})$  is modeled using a single GP fit to the data  $\mathcal{D} = \{(\mathbf{d}_i, \mathbf{z}_i, y_i)\}_{i=1}^n$ , where  $y_i = f(\mathbf{d}_i, \mathbf{z}_i) + \epsilon_i$  with  $\epsilon_i \sim N(0, \sigma_y^2)$ , which allows information to be borrowed across strata. One possible method of incorporating the additional covariates into the GP model is through the kernel function. We use an anisotropic squared exponential kernel function that includes the additional covariates of interest:

$$\mathcal{K}((\mathbf{d}, \mathbf{z}), (\mathbf{d}', \mathbf{z}')) = \sigma_f^2 \exp \left\{ - \left( \sum_{j=1}^J \frac{(d_j - d'_j)^2}{2l_{d_j}^2} + \sum_{p=1}^P \frac{(z_p - z'_p)^2}{2l_p^2} \right) \right\}. \quad (3)$$

As before, we use an empirical Bayes approach for estimating the hyperparameters  $\boldsymbol{\theta} = \{\sigma_f^2, \dots, l_P\}$ . In the case where  $Z_p$  is a binary variable representing the levels of covariate  $p$ , the correlation between two patient responses is reduced by a factor of  $\exp(-1/(2l_p^2))$  if they belong to different strata with respect to covariate  $p$ .

Since the objective function may exhibit different behavior within each stratum, each stratum may have a unique best objective function value  $f_k^*$ . Similar to the standard case,  $f_k^*$  is estimated as the minimum of the GP posterior mean surface within stratum  $k$ ,  $f_k^* = \min_{\mathbf{d}} \tilde{\boldsymbol{\mu}}(\mathbf{d}, \mathbf{z}_k)$ . To account for this heterogeneity, the sequential selection is performed within each stratum but with the GP fit utilizing data from all strata. This proceeds by modifying the EI acquisition function to use  $f_k^*$  when conditioned on being in stratum  $k$ , denoted by  $\alpha_{EI}(\tilde{\mathbf{d}} \mid \mathcal{D}, \tilde{\mathbf{z}}_k)$ . The sequential procedure continues until sample size limits are reached or until an early stopping rule is satisfied for each stratum. Since optimal doses in some strata may be easier to identify than in others, stratum-specific early stopping should be employed. One possible stratum specific stopping rule, which we denote by  $\mathbf{1}_{\text{STOP},k}$ , replaces  $n$  and  $\alpha_{EI}(\tilde{\mathbf{d}} \mid \mathcal{D})$  in (2) with  $n_k$  and  $\alpha_{EI}(\tilde{\mathbf{d}} \mid \mathcal{D}, \tilde{\mathbf{z}}_k)$ , respectively. Upon termination of the algorithm, the posterior distribution of the optimal dose combination for each strata is returned, denoted by  $p(\mathbf{d}_{opt} \mid \mathcal{D}, \mathbf{z}_k)$ . These modifications suggest Algorithm 2, referred to as the *personalized optimization algorithm*.

---

**Algorithm 2** Personalized Optimization Algorithm

---

**Require:**  $r$  patient responses at each of  $c$  initial dose combinations per stratum,  
 $\mathcal{D} = \{(\mathbf{d}_i, \mathbf{z}_i, y_i)\}_{i=1}^{n_0}$

- 1:  $n \leftarrow n_0 = \sum_{k=1}^K n_{0,k}$
- 2: Obtain  $p(\mathbf{f} \mid \mathcal{D}, \tilde{\mathbf{D}}, \tilde{\mathbf{Z}})$  using fitted GP ▷ Obtain posterior of  $f$
- 3: **for**  $k = 1, \dots, K$  **do**
- 4:     Obtain  $p(\mathbf{d}_{opt} \mid \mathcal{D}, \mathbf{z}_k)$  ▷ Obtain posterior of  $\mathbf{d}_{opt}$
- 5:      $f_k^* \leftarrow \min_{\mathbf{d}} \tilde{\boldsymbol{\mu}}(\mathbf{d}, \mathbf{z}_k)$  ▷ Obtain best value  $f_k$
- 6:     Calculate  $\alpha_{EI}(\tilde{\mathbf{d}} \mid \mathcal{D}, \tilde{\mathbf{z}}_k)$  for  $\tilde{\mathbf{d}} \in \mathbb{D}$  ▷ Compute EI
- 7:      $\mathbb{1}_{STOP,k} \leftarrow \text{FALSE}$
- 8: **end for**
- 9: **while**  $n < N$  and  $\mathbb{1}_{STOP,k} = \text{FALSE}$  for at least one stratum  $k$  **do**
- 10:     **for**  $k = 1, \dots, K$  **do**
- 11:          $n_k \leftarrow 0$
- 12:          $\mathcal{D}_k = \emptyset$
- 13:         **if**  $\mathbb{1}_{STOP,k} = \text{FALSE}$  **then**
- 14:              $\mathbf{d}^{(c_k+1)} \leftarrow \operatorname{argmax}_{\tilde{\mathbf{d}} \in \mathbb{D}} \alpha_{EI}(\tilde{\mathbf{d}} \mid \mathcal{D}, \tilde{\mathbf{z}}_k)$  ▷ Obtain next dose
- 15:             **for**  $i = 1, \dots, r$  **do**
- 16:                 Evaluate  $y_i$  at  $(\mathbf{d}^{(c_k+1)}, \mathbf{z}_k)$  ▷ Observe outcomes
- 17:             **end for**
- 18:              $n_k \leftarrow r$
- 19:              $\mathcal{D}_k = \{(\mathbf{d}_i^{(c_k+1)}, \mathbf{z}_k, y_i)\}_{i=1}^r$
- 20:             **end if**
- 21:         **end for**
- 22:          $n \leftarrow n + \sum_{k=1}^K n_k$  ▷ Update  $n$
- 23:          $\mathcal{D} = \mathcal{D} \cup \bigcup_{k=1}^K \mathcal{D}_k$  ▷ Update data
- 24:         Obtain  $p(\mathbf{f} \mid \mathcal{D}, \tilde{\mathbf{D}}, \tilde{\mathbf{Z}})$  using fitted GP ▷ Obtain posterior of  $f$
- 25:         **for**  $k = 1, \dots, K$  **do**
- 26:             Obtain  $p(\mathbf{d}_{opt} \mid \mathcal{D}, \mathbf{z}_k)$  ▷ Obtain posterior of  $\mathbf{d}_{opt}$
- 27:             **if**  $\mathbb{1}_{STOP,k} = \text{FALSE}$  **then**
- 28:                  $f_k^* \leftarrow \min_{\mathbf{d}} \tilde{\boldsymbol{\mu}}(\mathbf{d}, \mathbf{z}_k)$  ▷ Obtain best value  $f_k$
- 29:                 Calculate  $\alpha_{EI}(\tilde{\mathbf{d}} \mid \mathcal{D}, \tilde{\mathbf{z}}_k)$  for  $\tilde{\mathbf{d}} \in \mathbb{D}$  ▷ Compute EI
- 30:                 Update  $\mathbb{1}_{STOP,k}$  using (2) ▷ Update stopping rule
- 31:             **end if**
- 32:         **end for**
- 33: **end while**

---

### 3 Simulation Study

Below we perform a simulation study to compare the performance of the standard and personalized algorithms (Algorithms 1 and 2, respectively) under three scenarios where we set  $\mathbb{1}_{STOP} = \text{FALSE}$  and  $\mathbb{1}_{STOP,k} = \text{FALSE}$  for all  $k$ , respectively (i.e., no early stopping). Early stopping will be investigated in the next section. Scenarios 1 and 2 consider a single binary covariate  $Z_1$ . We index

the true optimal dose combinations,  $\mathbf{d}_{opt,k}$ , and the true optimal values of the objective function,  $f_{opt,k}$ , using the values of  $Z_1$ . That is, when  $Z_1 = 0$  we use  $\mathbf{d}_{opt,0}$  and  $f_{opt,0}$ . Scenario 3 considers two binary covariates,  $Z_1$  and  $Z_2$ , and the  $\mathbf{d}_{opt,k}$  and  $f_{opt,k}$  are indexed similarly. For example, when  $Z_1 = 0$  and  $Z_2 = 1$ , we use  $\mathbf{d}_{opt,01}$  and  $f_{opt,01}$ . To make the simulations in this manuscript more computationally feasible, we modify Algorithms 1 and 2 to return a point estimate of  $\mathbf{d}_{opt,k}$  rather than the entire posterior distribution. The point estimate is defined as the minimizer of the posterior mean surface,  $\hat{\mathbf{d}}_{opt,k} = \operatorname{argmin}_{\mathbf{d}} \tilde{\boldsymbol{\mu}}(\mathbf{d}, \mathbf{z}_k)$ .

We utilize dose combinations  $\mathbf{d} = (d_1, d_2) \in [0, 1]^2$ , assumed to be standardized, where  $\mathbf{d} = (0, 0)$  corresponds to the combination using the lowest doses of interest for each agent and where  $\mathbf{d} = (1, 1)$  corresponds to the combination using the highest doses of interest for each agent. The point estimates,  $\hat{\mathbf{d}}_{opt,k}$ , and the next dose combinations for evaluation,  $\mathbf{d}^{(c_k+1)}$ , are set, respectively, as the minimizers of  $\tilde{\boldsymbol{\mu}}(\mathbf{d}, \mathbf{z}_k)$  and  $\alpha_{EI}(\tilde{\mathbf{d}} \mid \mathcal{D}, \tilde{\mathbf{z}}_k)$ , each of which is evaluated across an evenly spaced grid on  $[0, 1]^2$ . The grid is incremented by 0.01 in each dimension, reflecting the degree of precision to which the drug maker can manufacture a particular dose combination. As a result, some dose combinations may be suggested more than once in the algorithm. We note it is important that the optimization procedures incorporate any manufacturing constraints; otherwise, doses which are not feasible to engineer may be suggested for exploration.

As before, we define  $f^\dagger(\mathbf{d}, \mathbf{z})$  to be a continuous efficacy surface and assume we are in a minimal toxicity setting where it is ethically permissible to select future doses anywhere in the dose combination space. We define our objective function as the negative of the efficacy surface,  $f(\mathbf{d}, \mathbf{z}) = -f^\dagger(\mathbf{d}, \mathbf{z})$ . The objective functions under the considered scenarios use the following negative multivariate normal densities:

$$g_1(\mathbf{d}) = -N \left[ \begin{pmatrix} 1 \\ 0.5 \end{pmatrix}, \begin{pmatrix} 0.1 & 0 \\ 0 & 0.1 \end{pmatrix} \right] \quad g_2(\mathbf{d}) = -N \left[ \begin{pmatrix} 0.3 \\ 0.7 \end{pmatrix}, \begin{pmatrix} 0.2 & 0.05 \\ 0.05 & 0.1 \end{pmatrix} \right]$$

$$g_3(\mathbf{d}) = -N \left[ \begin{pmatrix} 0.7 \\ 0.3 \end{pmatrix}, \begin{pmatrix} 0.2 & 0.05 \\ 0.05 & 0.1 \end{pmatrix} \right].$$

The data generating mechanism for each scenario is  $y = f(\mathbf{d}, \mathbf{z}) + \epsilon$  where  $\epsilon \sim N(0, \sigma_y = 0.2)$ , with

Table 1: Simulation scenarios considered. The data generating mechanism for each scenario is  $y = f(\mathbf{d}, \mathbf{z}) + \epsilon$  where  $\epsilon \sim N(0, \sigma_y)$ .

	$f(\mathbf{d}, \mathbf{z})$	$\sigma_y$	$z_1$	$z_2$	$\mathbf{d}_{opt}$	$f_{opt}$
Simulation Study	1) $\mathbf{1}\{z_1 = 0\} \times g_1(\mathbf{d}) + \mathbf{1}\{z_1 = 1\} \times g_1(\mathbf{d})$	0.2	0		(1, 0.5)	-1.59
			1		(1, 0.5)	-1.59
	2) $\mathbf{1}\{z_1 = 0\} \times g_2(\mathbf{d}) + \mathbf{1}\{z_1 = 1\} \times g_3(\mathbf{d})$	0.2	0		(0.3, 0.7)	-1.20
			1		(0.7, 0.3)	-1.20
	3) $\mathbf{1}\{(z_1 = 0, z_2 = 0)\} \times 0 + \mathbf{1}\{(z_1 = 0, z_2 = 1)\} \times g_1(\mathbf{d})$ $+ \mathbf{1}\{(z_1 = 1, z_2 = 0)\} \times g_3(\mathbf{d}) + \mathbf{1}\{(z_1 = 1, z_2 = 1)\} \times g_2(\mathbf{d})$	0.2	0	0	None	None
			0	1	(1, 0.5)	-1.59
		1	0	(0.7, 0.3)	-0.60	
		1	1	(0.3, 0.7)	-1.20	
Implant <sup>a</sup>	$\mathbf{1}(z_1 = 0) \times h_1(\mathbf{d}) + \mathbf{1}(z_1 = 1) \times h_2(\mathbf{d}) - 2$	2	0		(0.3, 0.7)	-10
			2	1	(0.7, 0.3)	-7

a: The subtraction of 2 in  $f(\mathbf{d}, \mathbf{z})$  corresponds to a base level of drug response outside the regions of optimality.

the specification of  $f(\mathbf{d}, \mathbf{z})$  included in the first panel of Table 1 (rows labeled ‘‘Simulation Study’’) and plotted in panel A of Figures 1-3. The value of  $\sigma_y$  represents a moderately large amount of noise and is held fixed for all scenarios. Increasing  $\sigma_y$  will lead to a smaller signal to noise ratio and may decrease the performance of the algorithms.

Scenario 1 considers the case of no response heterogeneity across a binary covariate  $Z_1$ . Both the locations of the optimal dose combinations, and the optimal values of the objective function, are the same across the strata. That is,  $\mathbf{d}_{opt,0} = \mathbf{d}_{opt,1}$  and  $f_{opt,0} = f_{opt,1}$ . Scenario 2 considers response heterogeneity across  $Z_1$ , where the locations of the optimal dose combinations differ. Under this scenario,  $\mathbf{d}_{opt,0} \neq \mathbf{d}_{opt,1}$  but  $f_{opt,0} = f_{opt,1}$ . Scenario 3 considers heterogeneity across two binary covariates,  $Z_1$  and  $Z_2$ , where both the locations of the optimal dose combinations and the optimal values of the objective function differ across the strata. Thus,  $\mathbf{d}_{opt,ij} \neq \mathbf{d}_{opt,lm}$  for  $ij \neq lm$  and  $f_{opt,ij} \neq f_{opt,lm}$  for  $ij \neq lm$ . This scenario includes a zero stratum,  $(z_1 = 0, z_2 = 0)$ , which represents the covariate pattern of those who do not respond to the drug. We note that in this stratum,  $\mathbf{d}_{opt,00}$  and  $f_{opt,00}$  do not exist.

For each scenario, the standard and personalized algorithms are run using a maximum sample size of 80 participants. While this number is larger than many early phase trials might be in practice, our goal is to investigate the algorithms’ performance characteristics as the sample size increases. We defer the use of early stopping rules to the following section, but note that these will

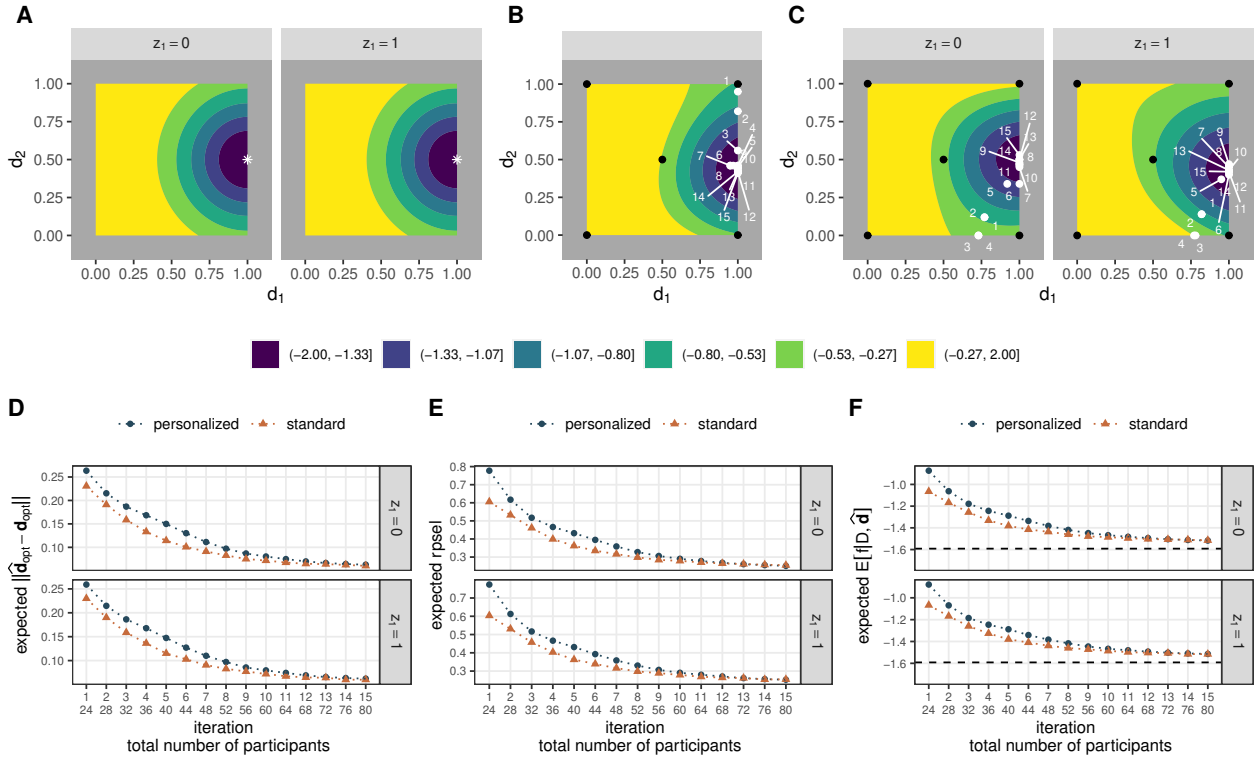


Figure 1: Scenario 1. A) Objective function, white stars denote  $\mathbf{d}_{opt,k}$ , B) single simulation using standard algorithm, C) single simulation using personalized algorithm, D) expected Euclidean distance as defined in (4) by iteration, E) expected RPSEL as defined in (5) by iteration, and F) expected posterior mean estimate by iteration. In (B) and (C), black points denote initial dose combinations and white points denote dose combinations evaluated at each iteration (labels may lie outside of dose combination range  $\mathbf{d} \in [0, 1]^2$ ). In (F), dashed lines for  $z_1 = 0$  and  $z_1 = 1$  are  $f_{opt,0} = f_{opt,1} = -1.59$ .

permit a reduction in the expected sample size. We assign participants to dose combinations such that the total sample size of each algorithm is equal at each iteration, which allows a comparison of their performance. For the standard algorithm under scenarios 1 and 2,  $r = 4$  participants are assigned to each dose combination on an initial dose matrix comprised of  $c = 5$  dose combinations,  $\mathbf{d} \in \{(0, 0), (0, 1), (0.5, 0.5), (1, 0), (1, 1)\}$ . More than one patient is assigned per dose combination to control the cost associated with producing novel dose-combinations, a financial constraint from our motivating problem. This yields  $n_0 = 20$ . At each iteration of the algorithm,  $r = 4$  additional participants are assigned to each proposed dose combination. This yields a total sample size of 80 after 15 iterations. We note that  $r$  is a tuning parameter, and that reducing it will lead to more unique doses being explored for the same fixed sample size. We explore this in the next section.

For the personalized algorithm, the same initial dose matrix of five points is used. To achieve the same total sample size by iteration as the standard algorithm, only  $r = 2$  participants are

assigned to each dose combination within each stratum. This yields  $n_{0,0} = n_{0,1} = 10$ , and so  $n_0 = 20$ , as in the standard algorithm. At each iteration within each stratum,  $r = 2$  additional participants are assigned to each proposed dose combination. This yields a total sample size of 80 after 15 iterations. The same setup is used for scenario 3. However, since the number of strata is doubled, the number of participants evaluated at each dose combination is halved for the personalized algorithm. Thus, the standard algorithm still evaluates  $r = 4$  participants per dose combination, but the personalized algorithm evaluates  $r = 1$  participant per dose combination, yielding a total sample size of 80 after 15 iterations.

For scenarios 1 and 2, examples of a single run of the standard and personalized algorithms are plotted in panels B and C of Figures 1 and 2, respectively. All computing is performed in the statistical programming language R (R Core Team, 2022). The objective functions are modeled using zero-mean GP models which utilize the anisotropic squared exponential kernels previously described, with the hyperparameters being jointly optimized by maximizing the marginal log-likelihood of the data (i.e., empirical Bayes GP; Gramacy 2016).

The performance of the algorithms is compared using several criteria which are estimated via  $m = 1, \dots, 1000$  Monte Carlo simulations. The expected Euclidean distance is used to assess how close the recommended dose combination  $\hat{\mathbf{d}}_k$  is to  $\mathbf{d}_{opt,k}$  at each iteration:

$$E_{y|z_k}[\|\hat{\mathbf{d}}_k - \mathbf{d}_{opt,k}\|] \approx \frac{1}{1000} \sum_{m=1}^{1000} \sqrt{(\hat{d}_1^{(m)} - d_{1,opt,k})^2 + (\hat{d}_2^{(m)} - d_{2,opt,k})^2}. \quad (4)$$

The expected root posterior squared error loss (RPSEL) is used to assess how well  $f_{opt,k}$  is estimated by the pointwise posterior distribution of the objective function at the recommended dose,  $p(f_k | \mathcal{D}, \hat{\mathbf{d}}_k, z_k)$ , where  $f^{(s)}(\hat{\mathbf{d}}_k, z_k)$  denotes a single posterior sample out of  $s = 1, \dots, 3000$  posterior samples:

$$E_{y|z_k}[\text{RPSEL}] \approx \frac{1}{1000} \sum_{m=1}^{1000} \left[ \frac{1}{3000} \sum_{s=1}^{3000} (f^{(s)}(\hat{\mathbf{d}}_k^{(m)}, z_k) - f_{opt,k})^2 \right]^{\frac{1}{2}}. \quad (5)$$

Finally, the expected posterior mean estimate  $E[f_k | \mathcal{D}, \hat{\mathbf{d}}_k, z_k]$  at each iteration is used to assess how quickly the point estimates converge to the true value of  $f_{opt,k}$ . Note that the standard algorithm ignores the strata and so yields only a single recommended dose  $\hat{\mathbf{d}}_k = \hat{\mathbf{d}}$ , posterior

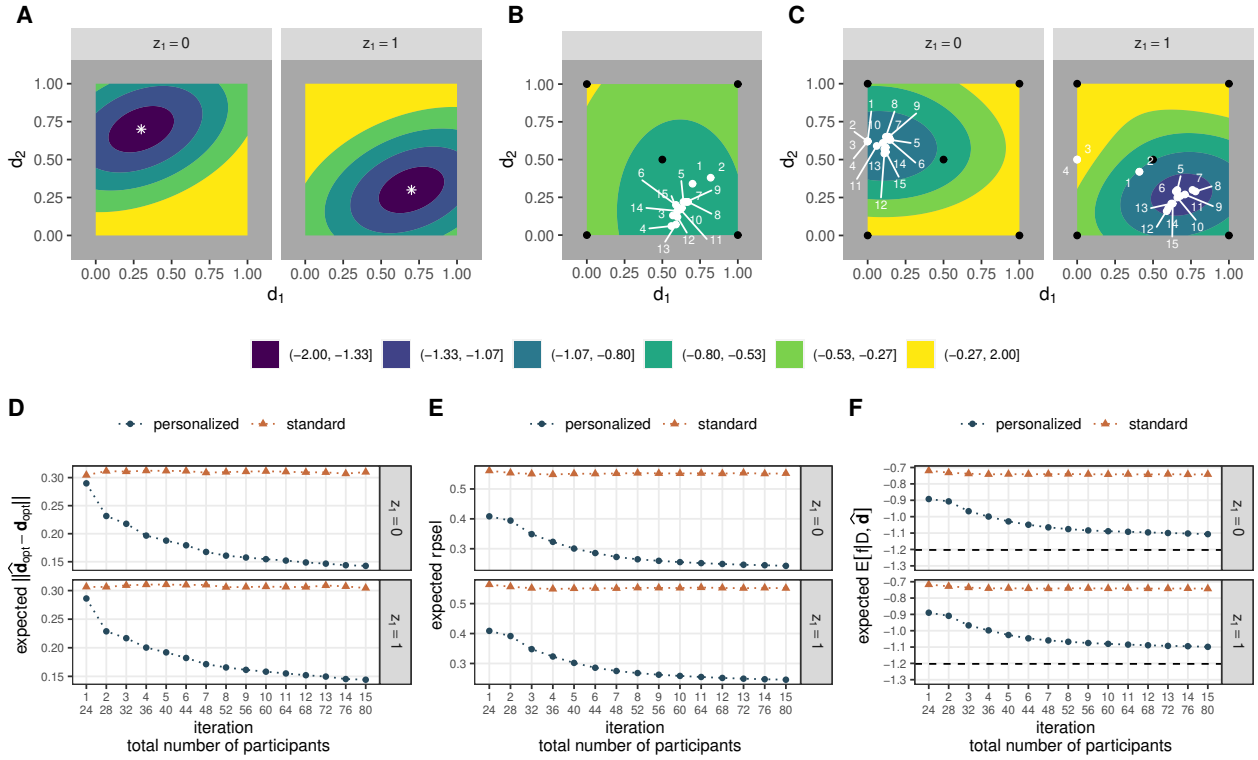


Figure 2: Scenario 2. A) Objective function, white stars denote  $\mathbf{d}_{opt,k}$ , B) single simulation using standard algorithm, C) single simulation using personalized algorithm, D) expected Euclidean distance as defined in (4) by iteration, E) expected RPSEL as defined in (5) by iteration, and F) expected posterior mean estimate by iteration. In (B) and (C), black points denote initial dose combinations and white points denote dose combinations evaluated at each iteration (labels may lie outside of dose combination range  $\mathbf{d} \in [0, 1]^2$ ). In (F), dashed lines for  $z_1 = 0$  and  $z_1 = 1$  are  $f_{opt,0} = f_{opt,1} = -1.20$ .

distribution  $p(f_k | \mathcal{D}, \hat{\mathbf{d}}_k, z_k) = p(f | \mathcal{D}, \hat{\mathbf{d}})$ , and posterior mean  $E[f_k | \mathcal{D}, \hat{\mathbf{d}}_k, z_k] = E[f | \mathcal{D}, \hat{\mathbf{d}}]$  per iteration for  $k = 1, \dots, K$ . Plots of these criteria by iteration are included in panels D-F of Figures 1 and 2 and panels B-D of Figure 3.

Scenario 1 considers the case of no response heterogeneity across binary covariate  $Z_1$ . Under this scenario, both algorithms converge to the locations of  $\mathbf{d}_{opt,k}$  and estimate the  $f_{opt,k}$  well (panels D-F of Figure 1). The personalized algorithm is slightly less efficient than the standard algorithm, however, and takes longer to converge. This may be explained by the GP model used in the personalized algorithm needing to estimate the additional length-scale parameter for  $Z_1$ ,  $l_1$ . Regardless, the performance of the two algorithms is comparable before their termination.

Scenario 2 considers response heterogeneity across  $Z_1$ . Under this scenario, the personalized algorithm converges to the locations of  $\mathbf{d}_{opt,k}$  and estimates the  $f_{opt,k}$  well, whereas the standard algorithm does not (panels D-F of Figure 2). In panel B of Figure 2, we see the standard algorithm

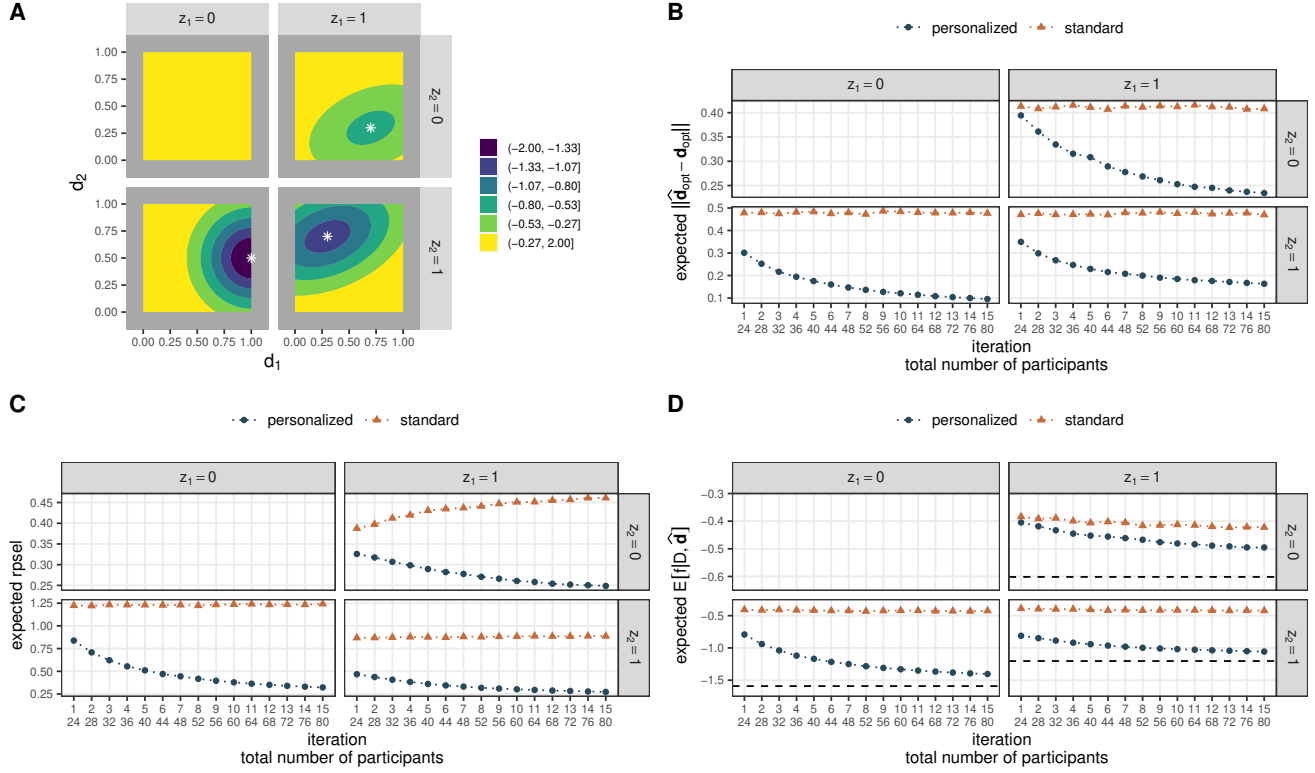


Figure 3: Scenario 3. A) Objective function, white stars denote  $\mathbf{d}_{opt,k}$ , B) expected Euclidean distance as defined in (4) by iteration, C) expected RPSEL as defined in (5) by iteration, and D) expected posterior mean estimate by iteration. In (B)-(D), the plots for  $(z_1 = 0, z_2 = 0)$  are empty as no optima exist. In (D), the dashed line for  $(z_1 = 0, z_2 = 1)$  is  $f_{opt,01} = -1.59$ , for  $(z_1 = 1, z_2 = 0)$  it is  $f_{opt,10} = -0.60$ , and for  $(z_1 = 1, z_2 = 1)$  it is  $f_{opt,11} = -1.20$ .

explores the area near only a single  $\mathbf{d}_{opt,k}$ , in this example  $\mathbf{d}_{opt,1}$ . Other times it explores the area near  $\mathbf{d}_{opt,0}$  or attempts to explore both optima. This results from the marginal objective function surface being bimodal, since it is a mixture distribution comprised of the equally weighted strata of  $Z_1$ , which are displayed in panel A of Figure 2. It is important to note that even if the bimodality of the marginal surface is properly identified and explored, patients cannot be optimally treated without consideration of  $Z_1$ . That is, without this additional covariate information, the standard algorithm cannot determine which mode should be used to treat patients with  $Z_1 = 0$  versus  $Z_1 = 1$ . This is easily handled using the personalized approach, however.

Scenario 3 considers heterogeneity across two binary covariates,  $Z_1$  and  $Z_2$ . Recall that the stratum  $(z_1 = 0, z_2 = 0)$  corresponds to those patients who do not respond to the drug. Thus there are no optima in this stratum and the corresponding plots in panels B-D of Figure 3 are empty. Under this scenario, the personalized algorithm converges to the locations of  $\mathbf{d}_{opt,k}$  and estimates

the  $f_{opt,k}$  well, whereas the standard algorithm does not (panels B-D of Figure 3). We note that convergence in the stratum ( $z_1 = 1, z_2 = 0$ ) is slower than in the others, potentially resulting from the optimal value of the objective function being smaller in magnitude, and thus the response surface is less peaked as compared to the other strata. Had an early stopping rule been employed here, and additional participants been available for enrollment, this stratum might continue to be explored after the algorithm had stopped in the others. This scenario suggests that as the number of strata grow, and thus also the likelihood for some degree of response heterogeneity to be present, the performance of the standard algorithm will be further degraded.

In summary, when heterogeneity exists across the strata, the personalized algorithm is superior in both identifying the locations of the  $\mathbf{d}_{opt,k}$  and estimating the  $f_{opt,k}$ . When no heterogeneity exists, the standard algorithm yields slightly better performance at earlier iterations only, with the personalized algorithm being comparable by the end of the trial. Finally, the personalized algorithm may explore the strata before settling on a region of optimality. This is most obvious in panel C of Figure 1, where the personalized algorithm initially explores regions away from  $\mathbf{d}_{opt,k}$  before eventually identifying the regions of optimality. This supports the notion that exploration of the objective function beyond the initial doses should be allowed before permitting early stopping. We consider this in the next section.

## 4 Dose-Finding Design for an Intraocular Implant

In this section we focus on the intraocular implant example. The goal is to develop an intraocular implant with an optimal dose combination of two agents which reduce intraocular pressure (IOP). The normal range of IOP is 12-21 mmHg, with 21-30 mmHg considered elevated IOP. Elevated IOP is a risk factor for ocular hypertension and glaucoma, and is strongly associated with increased vision loss (Leske et al., 2003). The implant seeks to reduce elevated IOP by combining two agents, with doses  $d_1$  and  $d_2$ , each of which has been in use individually in topical form for many years. The agents are well tolerated and we do not expect any drug-related events. We are interested in obtaining the optimal dose combination of these two agents using reduction in IOP from baseline as a continuous efficacy measure. It is hypothesized that higher doses do not necessarily imply greater

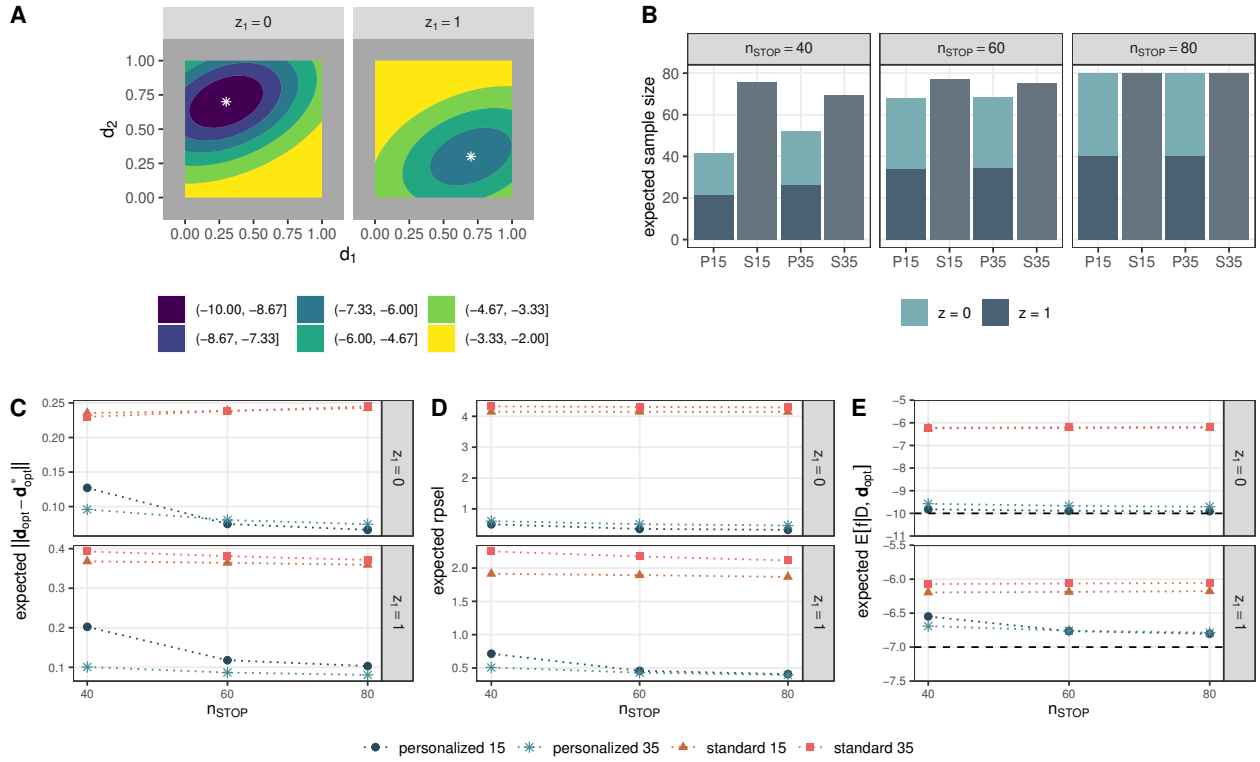


Figure 4: Intraocular Implant Scenario: A) Objective function, white stars denote  $\mathbf{d}_{opt,k}$ , B) expected sample size, C) expected Euclidean distance as defined in (4) by iteration, D) expected RPSEL as defined in (5) by iteration, and E) expected posterior mean estimate by iteration. On the x-axis in (B), P stands for personalized and S for standard, followed by the number of iterations. In (E), dashed line for  $z_1 = 0$  is  $f_{opt,0} = -10$  and for  $z_1 = 1$  is  $f_{opt,1} = -7$ .

efficacy, which is expected to plateau or even decrease at higher levels of agent concentration. Additionally, we expect response heterogeneity to exist with respect to a particular characteristic of the lens of the eye, which we treat as a binary covariate  $Z_1$ , and are interested in a design which permits identification of potentially different optimal dose combinations according to this patient characteristic.

We allow the dose-finding algorithm to explore the entire continuous dose-combination region, assumed to be standardized, and deem it ethically permissible to explore the dose combination region without safety escalation/de-escalation rules. It is hypothesized that the implant can reduce elevated IOP by 10 mmHg in individuals with  $Z_1 = 0$ , but may be less effective in individuals with  $Z_1 = 1$ . In these individuals, the reduction may be only 7 mmHg. To assess the cost and size of a hypothetical trial, we are interested in comparing the standard and personalized dosing approaches under different stopping rule specifications for the scenario described above. The final design is

then selected as the one which balances good performance while controlling expected cost. Costs are measured in terms of enrolled participants and also the number of unique dose combinations, since there are engineering costs associated with production of novel doses.

The goal is to minimize the objective function which, under the considered scenario, utilizes the following scaled negative multivariate normal densities:

$$h_1(\mathbf{d}) = -6.65N \left[ \begin{pmatrix} 0.3 \\ 0.7 \end{pmatrix}, \begin{pmatrix} 0.2 & 0.05 \\ 0.05 & 0.1 \end{pmatrix} \right] \quad h_2(\mathbf{d}) = -4.16N \left[ \begin{pmatrix} 0.7 \\ 0.3 \end{pmatrix}, \begin{pmatrix} 0.2 & 0.05 \\ 0.05 & 0.1 \end{pmatrix} \right].$$

The data generating mechanism for the scenario is  $y = f(\mathbf{d}, z) + \epsilon$  where  $\epsilon \sim N(0, \sigma_y = 2)$ , with the specification of  $f(\mathbf{d}, z)$  included in the second panel of Table 1 (row labeled ‘‘Implant’’) and plotted in panel A of Figure 4. We use the same indexing for  $\mathbf{d}_{opt,k}$  and  $f_{opt,k}$  as described previously. The value of  $\sigma_y$  is hypothesized to be a realistic measure of outcome variability for the implant.

Two settings of the algorithms are run for each scenario: one which allows for 15 total iterations, and one which allows for 35 total iterations, where both have a maximum sample size of 80 participants. We denote the standard algorithm under 15 and 35 iterations by  $S15$  and  $S35$ , respectively. We denote the personalized algorithm under 15 and 35 iterations as  $P15$  and  $P35$ , respectively. Under the first setting with a maximum of 15 iterations,  $S15$  and  $P15$  are run under the same specifications described in the previous section, where  $r = 4$  and  $r = 2$ , respectively. Under the second setting with a maximum of 35 iterations,  $S35$  and  $P35$  are run, respectively, with  $r = 2$  and  $r = 1$  for the same  $c = 5$  initial dose combinations described in the previous section.

As the sponsor is concerned about cost and size of the trial, early stopping is permitted using the rule defined in (2). Early stopping is investigated for  $n_{STOP} = 40$  and  $n_{STOP} = 60$  and is compared to the performance of no early stopping where  $n_{STOP} = 80$ . The values of  $\delta$  are determined through Monte Carlo as previously described. For  $n_{STOP} = 40$ ,  $\delta$  is set as 0.11, 0.33, 0.081, and 0.38 for algorithms  $P15$ ,  $S15$ ,  $P35$ , and  $S35$ , respectively. For  $n_{STOP} = 60$ ,  $\delta$  is set as 0.082, 0.36, 0.080,

and 0.38 for algorithms  $P15$ ,  $S15$ ,  $P35$ , and  $S35$ , respectively. Combining the three stopping rules (which includes no early stopping,  $n_{\text{STOP}} = 80$ ) with the two settings for the two algorithms yields 12 unique designs being compared. All computing and inference is performed as previously described. The performance of the algorithms is compared using the previously defined criteria which are estimated via 1,000 Monte Carlo simulations.

Under the scenario described above, the personalized algorithms yield similar performance except under  $n_{\text{STOP}} = 40$ , where  $P35$  yields dose combinations closer to  $\mathbf{d}_{\text{opt},k}$ , has comparable or smaller RPSEL, and yields comparable or better estimates of  $f_{\text{opt},k}$  (Figure 4, panels C-E). However, the  $P35$  algorithm has slightly higher expected sample sizes than  $P15$  (Figure 4, panel B). The standard algorithms perform very poorly, having inflated expected sample sizes, recommending dose combinations far from  $\mathbf{d}_{\text{opt},k}$ , having inflated RPSEL, and yielding posterior mean estimates which do not converge to  $f_{\text{opt},k}$  as compared to the personalized algorithms. We see that it may be beneficial to allow a larger number of unique doses to be explored, as better performance may be achieved earlier. A second scenario of no response heterogeneity was investigated, and conclusions are consistent with the finding in the simulation section, indicating reduced efficiency of the personalized algorithms (results not shown).

To select a final design (i.e., combination of stopping rule and maximum number of algorithm iterations), we use Figure 4 as a visual aide. Since response heterogeneity is expected a priori, the poor performance of the standard algorithms under this scenario makes them unusable in practice. Instead, we choose the personalized  $P35$  algorithm with  $n_{\text{STOP}} = 40$ . This design yields better performance than  $P15$  and has almost comparable performance as the same design with no early stopping (i.e.,  $P35$  for  $n_{\text{STOP}} = 80$ ). Choosing  $P35$  over  $P15$  does come with additional cost, however. Under this scenario where  $n_{\text{STOP}} = 40$ , the  $P15$  algorithm expects to evaluate about 16 unique dose combinations and enroll approximately 42 participants, whereas the  $P35$  algorithm expects to evaluate about 26 unique dose combinations and enroll approximately 52 participants. The sponsor deems the increased engineering and enrollment costs to be worth the increase in performance in this case.

## 5 Discussion

In this manuscript, we proposed the use of Bayesian optimization for early phase multi-agent dose-finding trials in a tolerated toxicity setting. We showed the benefit of taking a personalized approach for dual-agent trials when heterogeneity exists across a set of prespecified subgroups. As expected, under no response heterogeneity the personalized approach is slightly less efficient. As noted in the introduction, methods utilizing parametric models may suffer from the curse of dimensionality when transitioning from standard to personalized dose-finding, as they require terms for all higher order dose-covariate interactions. By using the anisotropic squared exponential GP kernel in the Bayesian optimization methods proposed here, however, only a single additional parameter per covariate is required (i.e., the additional lengthscale parameter corresponding to that covariate). Thus, the proposed methods help showcase the benefit and feasibility of adopting a personalized approach toward early phase multi-agent dose-finding trials.

The proposed approach is not without limitations. First, the methods proposed in this work assumed a tolerated toxicity across the dose combination space. Extension to higher-grade toxicity settings through incorporation of dose escalation/de-escalation remains as future work. Second, the personalized approach was demonstrated by considering dual-agent dose combinations in pre-defined subgroups only. Extension to dose combinations with more than two agents is trivial, but extension to continuous covariates without categorization is not trivial, and could be the subject of future investigations. When considering a larger number of dosing agents or covariates, space filling designs should be utilized to select the initial dose combinations to ensure adequate coverage of each stratum (Stein, 1987; McKay et al., 1979; Carnell, 2022). Existing space-filling design algorithms may not be readily applicable within a dose optimization context and further developments may be required. Third, the performance of the algorithms was assessed under a single level of noise only. Future work should investigate performance under different levels of noise. Another direction for future development is to extend the proposed approach to binary and ordinal outcomes where the proposed response models may be defined over a latent continuous surface. Finally, development of more robust stopping criteria may improve the efficiency of the optimization algorithms.

In this manuscript, Bayesian optimization is utilized as a global optimizer. While other global optimization methods exist (e.g., genetic algorithms and simulated annealing), they require many function evaluations and are thus not appropriate for early phase dose-finding trials where evaluations are expensive (Bull, 2011; Tracey and Wolpert, 2018). We employed the EI acquisition function under a GP surrogate model. Performance of the algorithms under different acquisition functions, surrogate models, and/or kernel functions should be investigated. The anisotropic kernel used in this work assumes that all strata have the same correlation structure and that the covariance between points in different strata are changed by a multiplicative factor only, which may not be true. Additionally, if the number of included covariates is large and there is reason to believe that only low level interactions between the drug combinations and covariates exist, different surrogate models could be employed, such as additive GPs (Duvenaud et al., 2011) or Bayesian additive regression trees (BART; Chipman et al. 2010). We assumed the dose-efficacy surface could be reasonably modeled using a stationary kernel. Since departures from stationarity could be present throughout the dose-response space, future work should investigate relaxing this assumption through use of non-stationary kernels or deep GPs (Sauer et al., 2023).

Finally, we adopted an empirical Bayes approach toward the GP hyperparameter estimation to decrease the computational burden of the simulations. Likelihood methods can yield poor results when the sample sizes are small, as in early phase dose-finding trials, and so full Bayesian inference may be preferred (Bull, 2011; Wang and de Freitas, 2014). Unfortunately, the Markov chain Monte Carlo methods typically used to perform full Bayesian inference are prohibitively expensive for the algorithms proposed here, and so a sequential Monte Carlo approach may be a less computationally demanding alternative (Gramacy and Polson, 2011).

## Data Availability

No new data were created or analyzed in this study. The R scripts used for the simulations and graphics can be found on a public GitHub repository at [https://github.com/jjwillard/bayesopt\\_pers\\_df](https://github.com/jjwillard/bayesopt_pers_df).

## Acknowledgements

JW acknowledges the support of a doctoral training scholarship from the Fonds de recherche du Québec - Nature et technologies (FRQNT) and a research exchange internship with PharmaLex Belgium. SG acknowledges the support by a Discovery Grant from the Natural Sciences and Engineering Research Council of Canada (NSERC) and a Chercheurs-boursiers (Junior 1) award from the Fonds de recherche du Québec - Santé (FRQS). EEMM acknowledges support from a Discovery Grant from NSERC. EEMM is a Canada Research Chair (Tier 1) in Statistical Methods for Precision Medicine and acknowledges the support of a chercheur de mérite career award from the FRQS. This research was enabled in part by support provided by Calcul Québec and the Digital Research Alliance of Canada.

## References

- Berry, S. M., Carlin, B. P., Lee, J. J., and Muller, P. (2010). *Bayesian Adaptive Methods for Clinical Trials*. CRC Press, Boca Raton, FL.
- Bull, A. D. (2011). Convergence Rates of Efficient Global Optimization Algorithms. *Journal of Machine Learning Research*, 12(88):2879–2904.
- Cai, C., Yuan, Y., and Ji, Y. (2014). A Bayesian Dose-Finding Design for Oncology Clinical Trials of Combinational Biological Agents. *Journal of the Royal Statistical Society. Series C, Applied Statistics*, 63(1):159.
- Carnell, R. (2022). *lhs: Latin Hypercube Samples*. R package version 1.1.5.
- Chipman, H. A., George, E. I., and McCulloch, R. E. (2010). BART: Bayesian Additive Regression Trees. *The Annals of Applied Statistics*, 4(1):266–298.
- Duque, D. R., Stephens, D. A., and Moodie, E. E.M. (2022). Estimation of Optimal Dynamic Treatment Regimes using Gaussian Process Emulation. *arXiv preprint arXiv:2105.12259*.
- Duvenaud, D. K., Nickisch, H., and Rasmussen, C. (2011). Additive Gaussian Processes. *arXiv preprint arXiv:1112.4394*.
- Freeman, N. L., Browder, S. E., McGinige, K. L., and Kosorok, M. R. (2022). Dynamic Treatment Regime Characterization via Value Function Surrogate with an Application to Partial Compliance. *arXiv preprint arXiv:2212.00650*.
- Garnett, R. (2023). *Bayesian Optimization*. Cambridge University Press, Cambridge, UK.
- Gramacy, R. B. (2016). laGP: Large-Scale Spatial Modeling via Local Approximate Gaussian Processes in R. *Journal of Statistical Software*, 72(1):1–46.
- Gramacy, R. B. (2020). *Surrogates: Gaussian Process Modeling, Design and Optimization for the Applied Sciences*. Chapman Hall/CRC, Boca Raton, FL. <http://bobby.gramacy.com/surrogates/>.

- Gramacy, R. B. and Lee, H. K. H. (2010). Optimization Under Unknown Constraints. *arXiv preprint arXiv:1004.4027*.
- Gramacy, R. B. and Polson, N. G. (2011). Particle Learning of Gaussian Process Models for Sequential Design and Optimization. *Journal of Computational and Graphical Statistics*, 20(1):102–118.
- Guo, B. and Zang, Y. (2022). A Bayesian Phase I/II Biomarker-based Design for Identifying Subgroup-Specific Optimal Dose for Immunotherapy. *Statistical Methods in Medical Research*, 31(6):1104–1119.
- Hirakawa, A., Wages, N. A., Sato, H., and Matsui, S. (2015). A Comparative Study of Adaptive Dose-Finding Designs for Phase I Oncology Trials of Combination Therapies. *Statistics in Medicine*, 34(24):3194–3213.
- Houede, N., Thall, P. F., Nguyen, H., Paoletti, X., and Kramar, A. (2010). Utility-Based Optimization of Combination Therapy Using Ordinal Toxicity and Efficacy in Phase I/II Trials. *Biometrics*, 66(2):532–540.
- Jones, D. R., Schonlau, M., and Welch, W. J. (1998). Efficient Global Optimization of Expensive Black-Box Functions. *Journal of Global Optimization*, 13(4):455–492.
- Leske, M. C., Heijl, A., Hussein, M., Bengtsson, B., Hyman, L., Komaroff, E., Group, E. M. G. T., et al. (2003). Factors for Glaucoma Progression and the Effect of Treatment: the Early Manifest Glaucoma Trial. *Archives of Ophthalmology*, 121(1):48–56.
- Li, D. H., Whitmore, J. B., Guo, W., and Ji, Y. (2017). Toxicity and Efficacy Probability Interval Design for Phase I Adoptive Cell Therapy Dose-Finding Clinical Trials. *Clinical Cancer Research*, 23(1):13–20.
- Lyu, J., Ji, Y., Zhao, N., and Catenacci, D. V. (2019). AAA: Triple Adaptive Bayesian Designs for the Identification of Optimal Dose Combinations in Dual-Agent Dose Finding Trials. *Journal of the Royal Statistical Society. Series C, Applied Statistics*, 68(2):385–410.

- McKay, M. D., Beckman, R. J., and Conover, W. J. (1979). A Comparison of Three Methods for Selecting Values of Input Variables in the Analysis of Output from a Computer Code. *Technometrics*, 21(2):239–245.
- Mozgunov, P., Cro, S., Lingford-Hughes, A., Paterson, L. M., and Jaki, T. (2022). A Dose-Finding Design for Dual-Agent Trials with Patient-Specific Doses for One Agent with Application to an Opiate Detoxification Trial. *Pharmaceutical Statistics*, 21(2):476–495.
- Murphy, K. P. (2023). *Probabilistic Machine Learning: Advanced Topics*. MIT Press, Cambridge, MA.
- Picheny, V., Ginsbourger, D., Richet, Y., and Caplin, G. (2013). Quantile-Based Optimization of Noisy Computer Experiments with Tunable Precision. *Technometrics*, 55(1):2–13.
- R Core Team (2022). *R: A Language and Environment for Statistical Computing*. R Foundation for Statistical Computing, Vienna, Austria.
- Sauer, A., Gramacy, R. B., and Higdon, D. (2023). Active Learning for Deep Gaussian Process Surrogates. *Technometrics*, 65(1):4–18.
- Stein, M. (1987). Large Sample Properties of Simulations Using Latin Hypercube Sampling. *Technometrics*, 29(2):143–151.
- Tracey, B. D. and Wolpert, D. (2018). Upgrading from Gaussian Processes to Student’s t Processes. *arXiv preprint arXiv:1801.06147*.
- Wages, N. A. and Conaway, M. R. (2014). Phase I/II Adaptive Design for Drug Combination Oncology Trials. *Statistics in Medicine*, 33(12):1990–2003.
- Wang, K. and Ivanova, A. (2005). Two-Dimensional Dose Finding in Discrete Dose Space. *Biometrics*, 61(1):217–222.
- Wang, Z. and de Freitas, N. (2014). Theoretical Analysis of Bayesian Optimisation with Unknown Gaussian Process Hyper-Parameters. *arXiv preprint arXiv:1406.7758*.

Wang, Z., Zhang, J., Xia, T., He, R., and Yan, F. (2023). A Bayesian Phase I-II Clinical Trial Design to Find the Biological Optimal Dose on Drug Combination. *Journal of Biopharmaceutical Statistics*. (accepted) <https://pubmed.ncbi.nlm.nih.gov/37461311/>.

Williams, C. K. and Rasmussen, C. E. (2006). *Gaussian Processes for Machine Learning*. MIT Press, Cambridge, MA.